Japanese Journal of Applied Physics **53**, 04EH02 (2014) **REGULAR PAPER**
http://dx.doi.org/10.7567/JJAP.53.04EH02

An extremely high room temperature mobility of two-dimensional holes in a strained Ge quantum well heterostructure grown by reduced pressure chemical vapor deposition

Maksym Myronov, Christopher Morrison, John Halpin, Stephen Rhead, Catarina Casteleiro, Jamie Foronda, Vishal Ajit Shah, and David Leadley

Department of Physics, The University of Warwick, Coventry CV4 7AL, U.K.
E-mail: M.Myronov@warwick.ac.uk

Received September 22, 2013; accepted October 28, 2013; published online February 6, 2014

An extremely high room temperature two-dimensional hole gas (2DHG) drift mobility of 4230 $cm^2 V^{-1} s^{-1}$ in a compressively strained Ge quantum well (QW) heterostructure grown by an industrial type RP-CVD technique on a Si(001) substrate is reported. The low-temperature Hall mobility and carrier density of this structure, measured at 333 mK, are 777000 $cm^2 V^{-1} s^{-1}$ and 1.9×10^{11} cm^{-2}, respectively. These hole mobilities are the highest not only among the group-IV Si based semiconductors, but also among p-type III–V and II–VI ones. The obtained room temperature mobility is substantially higher than those reported so far for the Ge QW heterostructures and reveals a huge potential for further application of strained Ge QW in a wide variety of electronic and spintronic devices.

1. Introduction

Germanium, with its very high intrinsic hole and electron mobilities of 1900 and 3900 $cm^2 V^{-1} s^{-1}$ at room temperature, respectively, is the most promising candidate material to replace Si channels in future complementary metal oxide semiconductor (CMOS) devices. Adoption of Ge technology recently came closer to reality after demonstration of superior quality GeO_2 gate dielectric and very high electron and hole mobilities obtained near the GeO_2/Ge interface in bulk Ge metal oxide semiconductor field effect transistor (MOSFET) devices.[1)] Biaxial compressive strain further enhances the hole mobility in Ge. In practice, this is obtained by epitaxial growth of a compressively strained Ge epilayer, a few nanometers thick, on an underlying standard Si(001) substrate via an intermediate strain-relaxed SiGe buffer. The strain narrows the band gap of Ge and causes the appearance of a quantum well (QW) in the valence band. Holes confined in the strained Ge QW form a two-dimensional hole gas (2DHG) and have an increased mobility due both to their lower effective mass and reduced scattering factors in this material system. Indeed, very high room temperature 2DHG mobilities in the range 2400–3100 $cm^2 V^{-1} s^{-1}$, with carrier densities of $(5–41) \times 10^{11}$ cm^{-2} are routinely achieved in 20–25-nm-thick Ge QWs.[2–7)] At lower temperatures, i.e., below 10 K, much higher 2DHG mobilities in the range of $(0.03–1.1) \times 10^6$ $cm^2 V^{-1} s^{-1}$ with carrier densities of $(3–19) \times 10^{11}$ cm^{-2} have been obtained.[8–11)] Until recently, such extremely high mobility holes, have only been obtained in strained Ge QWs that were grown by solid-source molecular beam epitaxy (SS-MBE) or low-energy plasma-enhanced chemical vapor deposition (LEPE-CVD) techniques. However, there is great interest in creating such structures by a mass production technique such as reduced pressure chemical vapor deposition (RP-CVD). RP-CVD offers the major advantage of unprecedented wafer scalability and is nowadays routinely used by leading companies in the semiconductor industry to grow epitaxial layers on Si(001) wafers of up to 300 mm diameter. Recently we reported an ultra-high low-temperature (12 K) 2DHG mobility exceeding one million in a strained Ge QW heterostructures grown by RP-CVD.[11)]

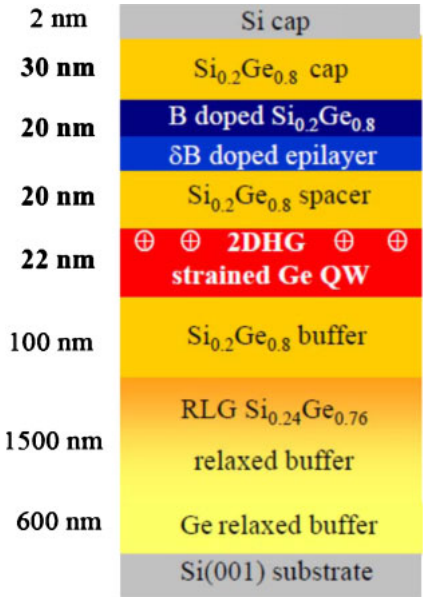

Fig. 1. (Color online) Schematic cross-section of a typical p-Ge QW MOD heterostructure grown on Si(001) substrate by RP-CVD.

For the first time, we report extremely high room temperature 2DHG drift mobility obtained in a compressively strained Ge QW epilayers grown by the RP-CVD technique. This value substantially exceeds previously reported mobilities in Ge QWs.

2. Epitaxial growth of strained Ge QW heterostructures and their characterization

2.1 Epitaxial growth of strained Ge QW heterostructures by RP-CVD

Modulation doping (MOD) in semiconductor heterostructures is a commonly used technique to create mobile carriers in a QW and thereby assess the quality of the QW material without the added complication of forming a gate stack that would be needed in a production device. In this work, RP-CVD has been used to grow entire p-type Ge QW MOD heterostructures. A schematic cross-section of a typical high mobility structure is shown in Fig. 1. The epilayers were

grown on 100 mm Si(001) substrates in an industrial type ASM Epsilon 2000 CVD system, which is a horizontal, cold wall, single wafer, load-lock reactor with a lamp heated graphite susceptor in a quartz tube. The structure consists of a ~600 nm relaxed Ge buffer, ~1500 nm reverse linearly graded (RLG) strain-relaxed $Si_{0.24}Ge_{0.76}$ buffer, an ~100 nm undoped $Si_{0.2}Ge_{0.8}$ buffer, a 22 nm undoped compressive strained Ge QW layer, a 20 nm undoped $Si_{0.2}Ge_{0.8}$ spacer layer, a Boron delta layer, a 20 nm boron doped $Si_{0.2}Ge_{0.8}$ supply layer, a 30 nm undoped SiGe cap layer, and ~2 nm Si cap epilayer on the surface. The Ge QW epilayers were grown using the common germane (GeH_4) precursor. The relatively thin, high Ge content SiGe/Ge buffer demonstrates good structural properties, i.e., relatively low root mean square (RMS) surface roughness of −2 nm and low threading dislocation density of $\sim 2 \times 10^6\,cm^{-2}$.[12,13] These properties make it an excellent global strain tuning platform for epitaxial growth of high quality Ge QW epilayers.

2.2 Characterization techniques

Cross-sectional transmission electron microscopy (XTEM) was performed using a JEOL 2000FX with an acceleration voltage of 200 kV. Samples were prepared for XTEM using mechanical lapping, then polished using a precision ion polisher. High resolution X-ray diffraction (HR-XRD) measurements were collected with a Panalytical XPert Pro Materials Reasearch Diffractometer equipped with a Ge(220) four-crystal monochromator and using Cu Kα_1 radiation ($\lambda = 1.540598$ Å). By using a Ge(220) analyzer before the detector the angular acceptance of the detector was reduced to 12 arcsec (triple axis configuration). The strain relaxation and Ge content in the SiGe epilayers were determined by HR-XRD reciprocal space maps (RSMs) around symmetrical (004) and asymmetrical (224) reflections. The surface roughness was measured by a Veeco multimode atomic force microscope (AFM) with a Nanonis controller in contact mode. Secondary ion mass spectrometry (SIMS) was used to obtain Ge, Si, B, and other impurities depth profiles in the researched heterostructures. Measurements were acquired using a near normal incidence O_2^+ and Cs primary beams at ultra-low energies of 250–500 eV. The Hall mobility and sheet carrier density of the heterostructures were obtained by a combination of resistivity and Hall effect measurements in the temperature range of 0.3–300 K. The data were obtained in the dark beginning at low temperatures. Hall bar devices, shown in Fig. 2, were fabricated in a clean room using optical lithography, metal evaporation and dry etching techniques. The Hall bar channel width is 50 µm and the separation between the nearest potential contacts is 250 µm. The Hall bar's mesa structure, including contacts area, was defined by dry etching down to the Si substrate. Hall mobility and carrier density as a function of temperature in the 10–300 K range were obtained in a closed cycle ^{4}He cryostat equipped with a 1.2 T electromagnet. Measurements were performed on Hall bar geometry devices with an applied current of 100 nA and magnetic field of <0.2 T. An Oxford Instruments Heliox AC-V ^{3}He cryostat was used to measure Hall mobility and carrier density, as well as magnetotransport up to 12 T at temperatures 0.3–300 K. In order to find out the transport properties of various carriers existing in multilayer semiconductor heterostructures, the magnetic-field dependence of magnetoresistance and Hall resistance have to be measured and the technique of mobility spectrum analysis (MSA) has to be applied. The magnetic-field dependence of the magnetoresistance and Hall resistance were measured as the magnetic field was swept continuously from −12 up to +12 T and reversed. The measured data were converted into conductivity tensor components [σ_{xx}(B) and σ_{xy}(B)] followed by a maximum-entropy MSA (ME-MSA) fitting procedure.[14] It is worth pointing out that the ME-MSA approach does not require any preliminary assumptions about the number of different types of carriers existing in a multilayer semiconductor heterostructure.

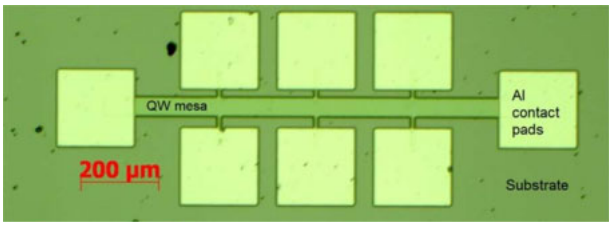

Fig. 2. (Color online) Optical microscope image of the Hall bar device fabricated for the magnetotransport measurements.

3. Results and discussion

Figure 3 shows the symmetrical (004) and asymmetrical (224) RSMs for the Ge QW heterostructure. All clearly visible peaks associated with various layers in the heterostructure are labelled therein. The slight misalignment between the substrate and the various layers of the Ge QW heterostructure along the [100] direction of the (004) RSM confirms the epilayers are slightly tilted with respect to the substrate. The Ge buffer layer is 105% relaxed with respect to the Si substrate (the layer is slightly tensile strained as a result of the difference in thermal contraction of both materials as they cool from the growth temperature) and the $Si_{0.24}Ge_{0.76}$ layer is 108% relaxed relative to the substrate. Subsequent layers grown on top of the $Si_{0.24}Ge_{0.76}$ epilayer are fully strained relative to it as denoted by the dashed line in the 224 RSM and shown in Fig. 3(b). These layers include $Si_{0.2}Ge_{0.8}$ in the buffer, spacer, Boron doped, and cap layers. The 22 nm Ge QW is under 0.8% lattice mismatch strain which is sufficiently enough to form a QW in the valence band and to create therein an energy sub-band(s) for 2DHG.

Bright field XTEM image of the entire Ge QW MOD heterostructure is shown Fig. 4(a). In the observed region, the dislocation network is confined in the Ge buffer and $Si_{0.24}Ge_{0.76}$ RLG buffer of the virtual substrate, with further growth being of good quality. The relaxed constant composition $Si_{0.24}Ge_{0.76}$ and $Si_{0.2}Ge_{0.8}$ buffer layers are free from visible defects which confirm low TDD (10^7–$10^8\,cm^{-2}$) in this material. The Fig. 4(b) shows bright field XTEM image of the Ge QW region. It confirms the thickness of the QW to be ~22 nm. It is very uniform and there is no indication of visible interface roughness. The bottom interface is abrupt and smooth, but the top one slightly smeared most likely due to Si and Ge intermixing at the interface. At 20 nm from the top interface there is a dark line which indicates the existence of a very thin SiGe epilayer due to Ge segregation during growth interrupt. Also this is the location

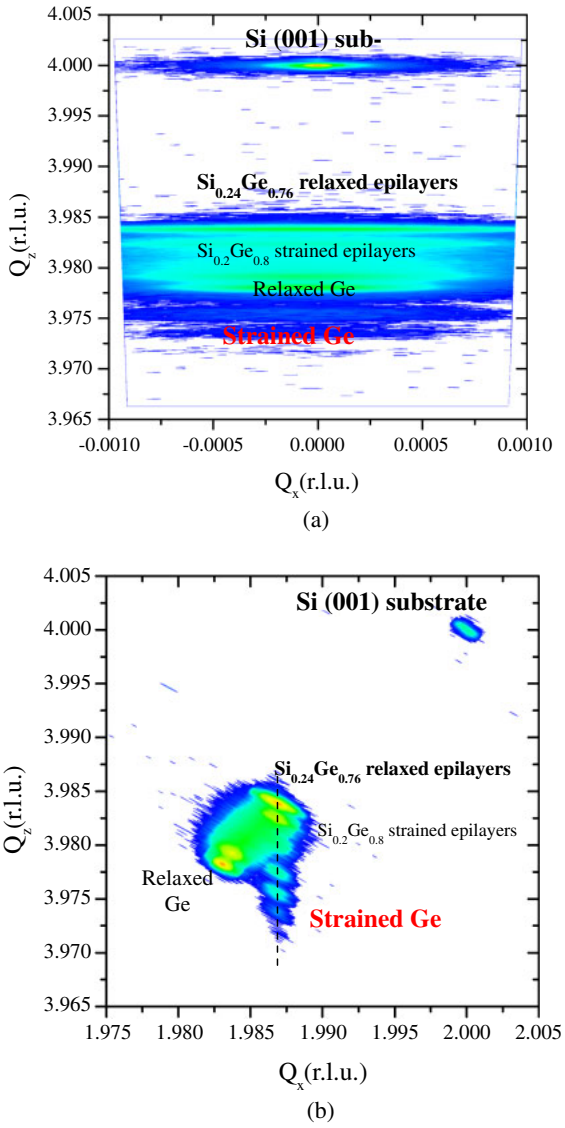

Fig. 3. (Color online) Symmetrical (004) (a) and asymmetrical (224) (b) RSMs of the Ge QW MOD heterostructure.

Fig. 4. (Color online) (a) Bright field XTEM of entire Ge QW MOD heterostructure. Dislocations can be seen to be confined to the graded region of the RLG buffer. (b) Bright field XTEM of the Ge QW region.

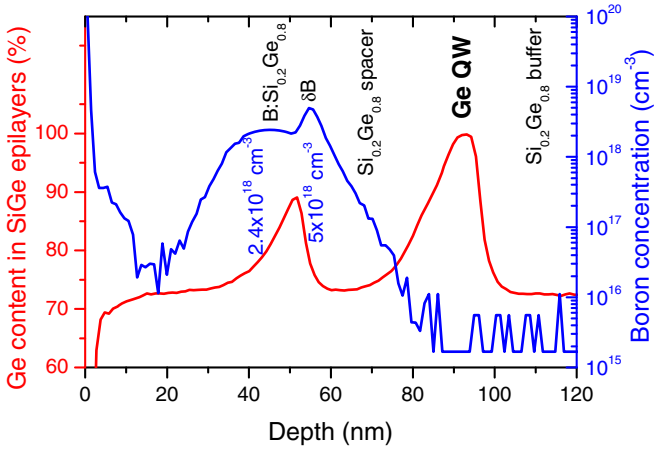

Fig. 5. (Color online) SIMS depth profiles of Boron and Ge in the modulation doped strained Ge QW region located close to the sample's surface.

of the Boron delta layer. The $Si_{0.2}Ge_{0.8}$ Boron doped and SiGe cap epilayers are clearly visible as well.

Multiple AFM scans acquired in different locations of the sample's surface reveal mean RMS surface roughness of 2.5 ± 0.5 nm. This is in good agreement with values obtained for the high Ge content SiGe/Ge/Si(001) RLG virtual substrates and Ge QW structures grown on top of them.[12,13,15,16] Also, surface morphology exhibits clear crosshatch pattern related to the strain field in the underlying epilayers caused by inhomogeneous distribution of misfit dislocations.

SIMS depth profiles of Boron and Ge in the modulation doped strained Ge QW region located close to the sample's surface are shown in the Fig. 5. A pure Ge QW is clearly visible. However, the right interface is more abrupt than the left one indicating some smearing of the Ge QW/$Si_{0.2}Ge_{0.8}$ spacer interface due to, most likely, Si and Ge intermixing occurring during epitaxial growth. There is another very narrow SiGe QW visible at the depth ~50 nm, is just above the Boron delta peak. The peak Ge concentration in this region is shown to be ~87%. This is a common feature and appears during growth interrupts due to Ge segregation under the given growth conditions. This typically leads to an increase in Ge content of a few percent which makes such epilayers visible even on XTEM images. However, in this sample it is much higher and appears to be due to enhanced Ge segregation by Boron delta doping. The profile also shows the Ge content in the SiGe epilayers to be ~73% instead of the expected 80% by design and and also confirmed by HR-XRD measurements. This Ge content discrepancy is acceptable for SIMS measurements in such SiGe heterostructures. The Boron concentration profiles agrees very well with those expected and consist of a Boron

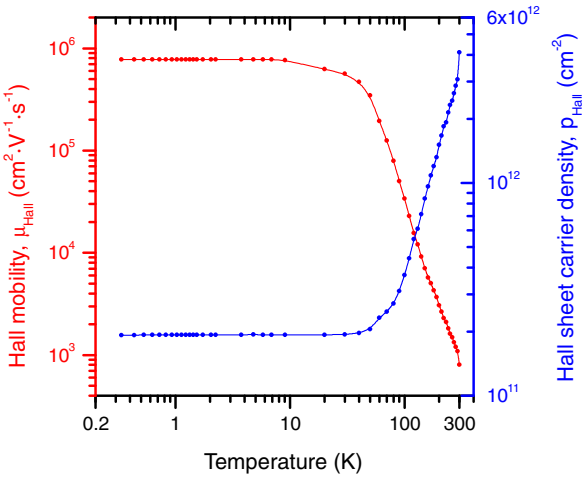

Fig. 6. (Color online) Temperature dependence of Hall mobility and Hall sheet carrier density for the strained Ge QW MOD heterostructure.

delta layer with a peak concentration of $5 \times 10^{18}\,cm^{-3}$ followed by a $Si_{0.2}Ge_{0.8}$ supply layer uniformly doped at $2.4 \times 10^{18}\,cm^{-3}$ with Boron. This layer sequence results in the remote supply of holes to the Ge QW and ensures a suppressed effect of the remote impurity scattering on 2DHG mobility in the Ge QW.

The Hall mobility and sheet carrier density of the 22 nm Ge QW MOD heterostructure were obtained by a combination of resistivity and Hall effect measurements on mesa-etched Hall-bar devices, as a function of temperature from 0.3 up to 300 K. The data are shown in Fig. 6. The sheet carrier density pronouncedly decrease from $\sim 4 \times 10^{12}\,cm^{-2}$ down to $\sim 2 \times 10^{11}\,cm^{-2}$ with decreasing temperature from 300 down to 50 K, respectively. This behavior is associated with freezing out of carriers in different epilayers of the heterostructure. It is most pronounced in the intentionally undoped SiGe, Ge and Si epilayers of the buffer, spacer and cap layers, which presumably contains very low concentrations of electrically active background impurities. At lower temperatures carrier density also reduces but substantially slower and almost saturates at $1.93 \times 10^{11}\,cm^{-2}$ at temperatures below 20 K. At the same time Hall mobility increases from ~ 800 up to $\sim 345000\,cm^2\,V^{-1}\,s^{-1}$ on reducing the temperature from 300 down to 50 K. Also, the Hall mobility still substantially increases up to $776000\,cm^2\,V^{-1}\,s^{-1}$ while the temperature is decreasing down to ~ 6 K. However in the case of Hall mobility, this increase is explained by the increase of the 2DHG drift mobility in the Ge QW due primarily to the reduction of phonon scattering. The temperature dependence described above of the Hall mobility and carrier density are typical for semiconductor QW structures in which all carriers freeze-out at low-temperatures and only 2D carriers in a QW exist. The low-temperature Hall mobility and carrier density of the Ge QW MOD heterostructure, measured at 333 mK, are $777000\,cm^2\,V^{-1}\,s^{-1}$ and $1.93 \times 10^{11}\,cm^{-2}$, respectively. However, in our case dopants in the Boron delta layer with peak concentration of $5 \times 10^{18}\,cm^{-3}$ must not freeze out even at low-temperatures and apparently there are carriers in the artificially created SiGe QW just above the Boron delta layer which also must exist at low-temperatures. These assumptions were confirmed by magnetotransport measurements at low-temperatures. Magnetic field dependence of Hall resistance (R_{xy}) and magnetoresistivity (ρ_{xx}) clearly show the presence of parallel conduction even at 333 mK. In this case we suppose the measured Hall mobility of $777000\,cm^2\,V^{-1}\,s^{-1}$ is an average mobility and does not correspond to the 2DHG in the 22 nm Ge QW. Also, it means 2DHG mobility could be substantially higher than $1.1 \times 10^6\,cm^2\,V^{-1}\,s^{-1}$ which we recently reported for similar type of 20 nm Ge QW MOD heterostructure without presence of any parallel conduction at low-temperatures.[11] Due to this we believe that 2DHG mobilities higher than the record 2DEG mobilities of $1.6 \times 10^6\,cm^2\,V^{-1}\,s^{-1}$ in strained Si QWs[17] could be obtained in Ge QW MOD heterostructures.

High temperature measurements and interpretation of the transport properties of any multilayered MOD semiconductor heterostructure are usually complicated by the existence of parallel conduction paths in doping supply layers, buffer layers and a substrate. The measured Hall mobility deviates to some degree from the drift mobility. At high temperatures parasitic parallel conduction paths are activated. In this case an average mobility and an average sheet carrier density arising from all conducting layers are measured by the Hall effect technique. A solution to this problem is to measure the magnetic field dependences of magnetoresistance and Hall resistance and to apply the technique of MSA.[14] The ME-MSA fit of magnetic-field dependence of conductivity tensor components, $\sigma_{xx}(B)$ and $\sigma_{xy}(B)$, measured at room temperature for the Ge QW MOD heterostructure is shown in Fig. 7(a). The fitted magnetic-field dependence of $\sigma_{xx}(B)$ and $\sigma_{xy}(B)$ are in very good agreement with the measured ones. Even visual analysis of the measured data clearly indicates the existence of strong parallel conduction in the heterostructure. The room temperature mobility spectrum as the result of conductivity tensor components $\sigma_{xx}(B)$ and $\sigma_{xy}(B)$ fits for the 22 nm Ge QW MOD heterostructure is shown in Fig. 7(b). The measured Hall mobility of $800\,cm^2\,V^{-1}\,s^{-1}$ is shown therein for clarity. The spectrum consists of four peaks. The highest mobility peak is attributed to the 2DHG in the strained 22 nm Ge QW. The drift mobility and sheet carrier density of the 2DHG extracted from the mobility spectrum are $4230\,cm^2\,V^{-1}\,s^{-1}$ and $1 \times 10^{11}\,cm^{-2}$ respectively. It is interesting to note that the contribution of 2DHG electrical conductivity is only $\sim 13\%$ to total conductivity of the Ge QW MOD heterostructure. This is mainly due to the substantial contribution to conductivity from the heavily Boron doped epilayers and intentionally undoped, but in reality containing some background impurities, relatively thick (comparing to just 22 nm Ge QW) SiGe epilayers.

The room temperature carrier density in the Ge QW was modeled by self-consistent 1D Poisson-Schrödinger simulation. The results are shown in Fig. 8. The epilayers structure was reconstructed taking into account the state of strain, dimensions and profiles obtained by HR-XRD, XTEM, and SIMS characterization techniques presented above. The valence energy-band diagram shows the existence of a 22 nm wide Ge QW with multiple energy sub-bands therein. The first two shown HH and LH correspond to the filled in heavy- and light-hole energy levels. Also, segregated Ge, above the Boron delta layer, is responsible for the formation of another narrow SiGe QW in the Boron doped

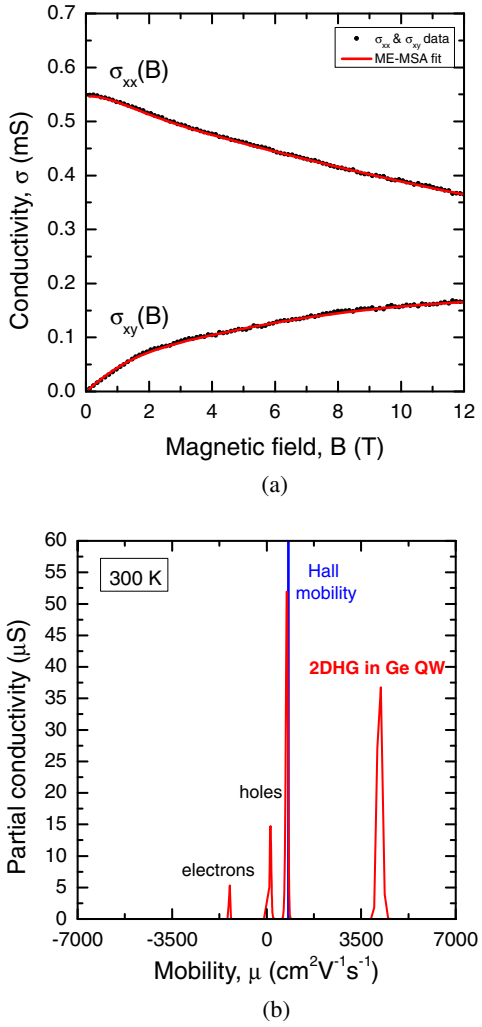

Fig. 7. (Color online) (a) The ME-MSA fit (solid lines) of magnetic-field dependence of conductivity tensor components, σ_{xx}(B) and σ_{xy}(B), measured at room temperature (circles) for the Ge QW MOD heterostructure. (b) Room temperature mobility spectrum as the result of conductivity tensor components σ_{xx}(B) and σ_{xy}(B) fits for the Ge QW MOD heterostructure. The measured Hall mobility is shown for clarity.

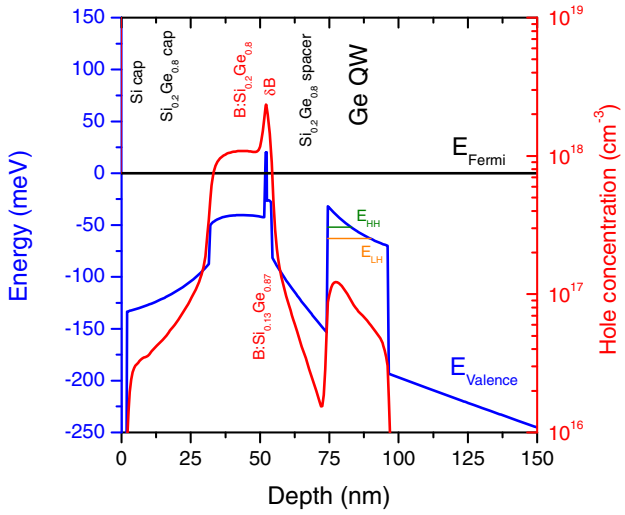

Fig. 8. (Color online) Valence energy-band diagram and hole concentration profile at 300 K for Ge QW MOD heterostructure obtained with the help of a self-consistent 1D Poisson-Schrödinger simulation. HH3 and LH3 corresponds to the filled in heavy- and light-hole energy levels in the 22 nm strained Ge QW.

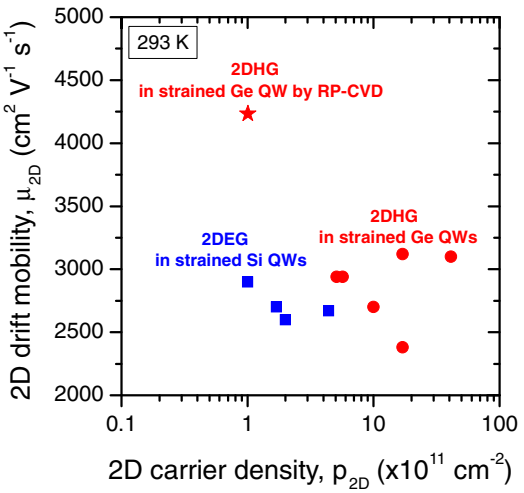

Fig. 9. (Color online) The highest 2DHG and 2DEG drift mobilities as a function of the carrier density at room temperature. The 2DHG mobilities in Ge QWs are shown by red circles. The 2DEG in Si QWs are shown by blue squares. The 2DHG obtained in this work is shown by red star.

region. This QW as well as Boron doped layers are responsible for the existence of large parallel conduction at room temperature demonstrated by results of the ME-MSA. The modelled hole concentration in the Ge QW is $1.7 \times 10^{11}\,\mathrm{cm}^{-2}$. This value is similar to that obtained by ME-MSA ($1 \times 10^{11}\,\mathrm{cm}^{-2}$) and could be different due to the uncertainty of modelling parameters or multiple energy levels population in the Ge QW. It is important to note that most of the holes in the Ge QW are located near the top Ge QW/$Si_{0.2}Ge_{0.8}$ spacer interface. Because of this, interface roughness scattering could be responsible for degradation of the 2DHG mobility.

A number of theoretical and experimental works on the analysis of 2DHG mobility in the SiGe heterostructures,[18–23] including the most recent one which contradicts even experimental 2DHG mobilities in strained Ge QWs published so far,[7] were carried out and published. Many of them predict the 2DHG drift mobility to be over $4000\,\mathrm{cm}^2\,\mathrm{V}^{-1}\,\mathrm{s}^{-1}$ at room temperature. However, complexity of calculations and the large number of variable parameters gave quite large scattering in the predicted values. In order to compare obtained results with previously reported ones the highest mobilities for 2DHG in compressive strained Ge QWs, grown by various approaches, and 2DEG in the tensile strained Si QWs along with the results obtained in this work are summarized in Fig. 9. The highest 2DHG mobilities of $3100\,\mathrm{cm}^2\,\mathrm{V}^{-1}\,\mathrm{s}^{-1}$ (at $4.1 \times 10^{12}\,\mathrm{cm}^{-2}$) and $3120\,\mathrm{cm}^2\,\mathrm{V}^{-1}\,\mathrm{s}^{-1}$ (at $1.7 \times 10^{12}\,\mathrm{cm}^{-2}$) were obtained in the 20 nm strained Ge QWs grown on $Si_{0.45}Ge_{0.55}$/S(001) or $Si_{0.35}Ge_{0.65}$/S(001) virtual substrates by SS-MBE.[7] Even though both mobilities are almost the same (especially taking into account measurements error) the carrier densities are different by approximately 2.5 times. The value of 2DHG mobility obtained here exceeds the highest previously reported one by over ~40%. In the past many works assumed a negligible effect of background ionized impurity scattering on room temperature 2DHG mobility. Indeed, both optical and acoustic phonon

scattering are the main mobility limiting factors at room temperature. Their mobilities are proportional to the effective width of a Ge QW. In this case mobilities in both samples have to be similar. Another mobility limiting factor which was very commonly assumed to exist in SiGe heterostructures is interface roughness scattering. In our RP-CVD heterostructures the Ge QW/$Si_{0.2}Ge_{0.8}$ spacer interface is smeared which could be considered as an enhanced interface roughness and/or stronger alloy scattering which both have to lead to substantial degradation of the mobility. However, by comparing these two structures grown by either RP-CVD or SS-MBE we believe the 2DHG drift mobility in the 22 nm strained Ge QW grown by RP-CVD to be mainly limited by background ionized impurity scattering. We also considered the remote ionized impurity scattering by ionized Boron dopants in the supply layers but it is very unlikely to be responsible for the demonstrated enhancement of the 2DHG mobility.

4. Conclusions

In conclusion, we report extremely high room temperature 2DHG mobility of 4230 $cm^2 V^{-1} s^{-1}$ in a compressively strained Ge QW grown by industrial type RP-CVD technique. The obtained mobility is substantially higher than those reported so far and grown by research type epitaxial growth techniques, i.e., SS-MBE and LEPE-CVD. Also, the room and low temperature holes mobilities are the highest not only among the group-IV Si based semiconductors, but also among p-type III–V and II–VI ones. This result demonstrates very high quality of the strained Ge QW epilayers grown by the RP-CVD and demonstrates the huge potential for further applications of such materials in CMOS, p-MOSFET and -MODFET devices on Si(001) or SOI(001) substrates.

Acknowledgement

This work was supported by the EPSRC funded “Spintronic device physics in Si/Ge Heterostructures” EP/J003263/1 and “Platform Grant” EP/J001074/1 projects.

1) K. Morii, T. Iwasaki, R. Nakane, M. Takenaka, and S. Takagi, IEEE Electron Device Lett. **31**, 1092 (2010).
2) M. Myronov, K. Sawano, Y. Shiraki, T. Mouri, and K. M. Itoh, Appl. Phys. Lett. **91**, 082108 (2007).
3) H. von Känel, D. Chrastina, B. Rössner, G. Isella, J. P. Hague, and M. Bollani, Microelectron. Eng. **76**, 279 (2004).
4) M. Myronov, T. Irisawa, O. A. Mironov, S. Koh, Y. Shiraki, T. E. Whall, and E. H. C. Parker, Appl. Phys. Lett. **80**, 3117 (2002).
5) R. J. H. Morris, T. J. Grasby, R. Hammond, M. Myronov, O. A. Mironov, D. R. Leadley, T. E. Whall, E. H. C. Parker, M. T. Currie, C. W. Leitz, and E. A. Fitzgerald, Semicond. Sci. Technol. **19**, L106 (2004).
6) H. von Känel, M. Kummer, G. Isella, E. Müller, and T. Hackbarth, Appl. Phys. Lett. **80**, 2922 (2002).
7) T. Tanaka, Y. Hoshi, K. Sawano, N. Usami, Y. Shiraki, and K. M. Itoh, Appl. Phys. Lett. **100**, 222102 (2012).
8) Y. H. Xie, D. Monroe, E. A. Fitzgerald, P. J. Silverman, F. A. Thiel, and G. P. Watson, Appl. Phys. Lett. **63**, 2263 (1993).
9) M. Myronov, K. Sawano, and Y. Shiraki, Appl. Phys. Lett. **88**, 252115 (2006).
10) B. Rössner, D. Chrastina, G. Isella, and H. von Känel, Appl. Phys. Lett. **84**, 3058 (2004).
11) A. Dobbie, M. Myronov, R. J. H. Morris, A. H. A. Hassan, M. J. Prest, V. A. Shah, E. H. C. Parker, T. E. Whall, and D. R. Leadley, Appl. Phys. Lett. **101**, 172108 (2012).
12) V. A. Shah, A. Dobbie, M. Myronov, D. J. F. Fulgoni, L. J. Nash, and D. R. Leadley, Appl. Phys. Lett. **93**, 192103 (2008).
13) V. A. Shah, A. Dobbie, M. Myronov, and D. R. Leadley, J. Appl. Phys. **107**, 064304 (2010).
14) S. Kiatgamolchai, M. Myronov, O. A. Mironov, V. G. Kantser, E. H. C. Parker, and T. E. Whall, Phys. Rev. E **66**, 036705 (2002).
15) M. Myronov, A. Dobbie, V. A. Shah, X.-C. Liu, V. H. Nguyen, and D. R. Leadley, Electrochem. Solid-State Lett. **13**, H388 (2010).
16) M. Myronov, K. Sawano, D. R. Leadley, and Y. Shiraki, Ext. Abstr. Solid State Devices and Materials (SSDM), 2010, p. K81.
17) T. M. Lu, D. C. Tsui, C.-H. Lee, and C. W. Liu, Appl. Phys. Lett. **97**, 059904 (2010).
18) B. Laikhtman and R. A. Kiehl, Phys. Rev. B **47**, 10515 (1993).
19) M. V. Fischetti and S. E. Laux, J. Appl. Phys. **80**, 2234 (1996).
20) S. Madhavi, V. Venkataraman, and Y. H. Xie, J. Appl. Phys. **89**, 2497 (2001).
21) S. Madhavi, V. Venkataraman, J. C. Sturm, and Y. H. Xie, Phys. Rev. B **61**, 16807 (2000).
22) M. Myronov, T. Irisawa, S. Koh, O. A. Mironov, T. E. Whall, E. H. C. Parker, and Y. Shiraki, J. Appl. Phys. **97**, 083701 (2005).
23) Y. Zhang, M. V. Fischetti, B. Sorée, W. Magnus, M. Heyns, and M. Meuris, J. Appl. Phys. **106**, 083704 (2009).